PROCEEDINGS OF SCIENCE

Construction and performance of 4-D CsI calorimeter for the $K_L \to \pi^0 \nu\bar{\nu}$ search of KOTO experiment

Katsushige Kotera[a,*]

on behalf of the KOTO collaboration

[a] *Osaka University, 1-1 Machikaneyama, Toyonaka, Japan*

E-mail: coterra@champ.hep.sci.osaka-u.ac.jp

A major background for the $K_L \to \pi^0 \nu\bar{\nu}$ search at the KOTO experiment is caused by neutrons generating two showers in the calorimeter made of 50 cm-long 2760 undoped CsI crystals stacked in a 1.9 m-diameter cylinder. Neutrons tend to have interactions deeper than photons. In 2018 we upgraded the calorimeter by installing 4080 silicon photomultipliers (SiPMs) on the front surface. Each crystal has been read out with a PMT on the back surface of the crystal. The depth and timing information on each shower are obtained by measuring the difference and the average of the timing of SiPM and PMT. A clear separation of gamma- and neutron-events was achieved in 2019 data. Less than 0.3 neutron background events are expected when we reach the Standard-Model sensitivity of $K_L \to \pi^0 \nu\bar{\nu}$.

40th International Conference on High Energy physics - ICHEP2020
July 28 - August 6, 2020
Prague, Czech Republic (virtual meeting)

*Speaker

PoS(ICHEP2020)749

1. Introduction

We are searching for a rare kaon decay $K_L \to \pi^0\nu\bar{\nu}$ at the J-PARC KOTO experiment [1]. This mode directly breaks CP symmetry with a small Standard-Model (SM) branching fraction, $(3.0 \pm 0.3) \times 10^{-11}$. Because the theoretical uncertainty of the branching fraction is small, 2%, a deviation of the measurement from the theoretical prediction provides clues to physics beyond the SM [2, 3].

The signature of $K_L \to \pi^0\nu\bar{\nu}$ decay is two gammas from a neutral pion decay with no other particles. The detector consists of the downstream calorimeter for gamma detection and hermetical veto counters surrounding the decay region. Figure 1(a) shows the KOTO detector, and (b) shows the lateral segmentation of the calorimeter made of undoped cesium iodide (CsI) crystals. Two sizes of CsI crystals were stacked in a 1.9 m-diameter cylinder: 1) small crystals, dimension of $2.5 \times 2.5 \times 50\,\mathrm{cm}^3$ and 2) large crystals, with $5.0 \times 5.0 \times 50\,\mathrm{cm}^3$. The central region of $1.8 \times 1.8\,\mathrm{m}^2$ consists of 2240 small crystals surrounded with 476 large crystals. PMTs are attached on the back surface of the CsI crystals.

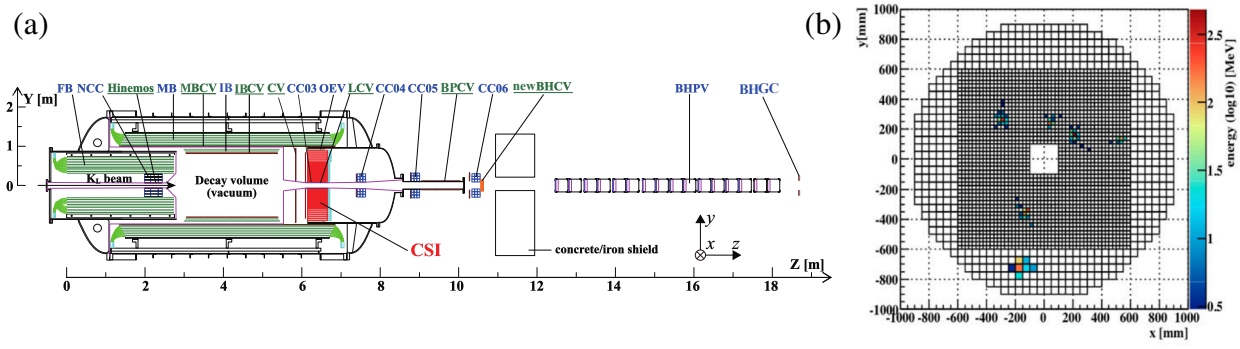

Figure 1: (a) Sectional side view of the KOTO detector. (b) Segmented view of the CsI calorimeter with six shower clusters from a $K_L \to 3\pi^0$ decay.

In our latest results a major background was caused by neutrons generating two showers in the calorimeter [1]. To reduce the neutron background, we discriminated the gamma shower cluster and the neutron shower cluster by using 1) pulse shape of signals and 2) cluster shape (CSD) in the CsI calorimeter. The estimated background level of neutron was 0.24 ± 0.17 at the single event sensitivity of $(1.30 \pm 0.01_{\mathrm{stat}} \pm 0.14_{\mathrm{syst}}) \times 10^{-9}$. This analysis clarified that we needed a new technique to reduce the neutron backgrounds by more than a factor of ten.

Neutrons tend to have interactions deeper than photons. The timing difference of scintillation light from the shower detected at the front side and the back side of CsI crystals reflects this position difference between neutrons and photons. We developed a technique to discriminate neutron events from gamma events by adding the SiPMs on the front surface.

The CSD uses the lateral shape of particle showers, and the new technique reported in this article uses the depth information of showers. Thus, we use three-dimensional information from the CsI calorimeter. The intrinsic time of showers is measured as an average of the timing from the front side and the back side. A neutron makes a hadronic shower, and another neutron produced in the primary shower propagates and makes a new shower in the calorimeter. Consequently, the second shower has a different timing from the first shower. This timing information is complementary to the depth information of showers. Thus, we use four-dimensional information from the CsI calorimeter.

To realize this 4-D calorimeter, we upgraded the CsI calorimeter by attaching 4080 silicon photomultipliers (SiPMs) on the front-end of the crystals in 2018. This article reports the technique to construct this 4-D calorimeter, and the background rejection capability with data taken in 2019.

2. Construction of the 4-D calorimeter

2.1 SiPM

We selected Hamamatsu MPPC S13360-6050CS[1] for the SiPMs. The usage of SiPM prevents an increase in the material budget mounted on the front surface of the CsI. The dimension of the package is $10.1 \times 8.9 \times 2.0\,\mathrm{mm}^3$ and the sensitive area is $6 \times 6\,\mathrm{mm}^2$ segmented in $50\,\mu$m pixels. The sensitive area is covered with silicone which is transparent to 310 nm scintillation light from CsI crystals.

The dark current of SiPM increases when they are irradiated by neutrons. In 2019, the SiPMs near the neutral beam had a large irradiation damage due to neutrons. It was estimated that the dark current of the SiPM closest to the neutral beam would increase by 10^3 times at the end of the KOTO experiment. However, we have tested this and concluded that the timing resolution of these SiPMs would be smaller than one nanosecond with a series of beam experiments. This timing resolution is sufficient to separate gamma and neutron events.

2.2 Readout method

As shown in Fig. 2(a), signals from four by four array of SiPMs were combined in an output signals as follows. Four SiPMs on neighboring four small crystals in the same row were read out together with a special circuit, and four of these signals in neighboring four rows were summed up in an amplifier [4]. These 4×4 of crystals make $10 \times 10\,\mathrm{cm}^2$ lateral area on the CsI calorimeter. Four SiPMs on a large crystal were read out together in the same way as for the four small crystals, and the signals from four large crystals were summed with an amplifier. These four large crystals were also grouped, making $10 \times 10\,\mathrm{cm}^2$ lateral area. This lateral area is comparable to the Molière radius of CsI, 3.5 cm.

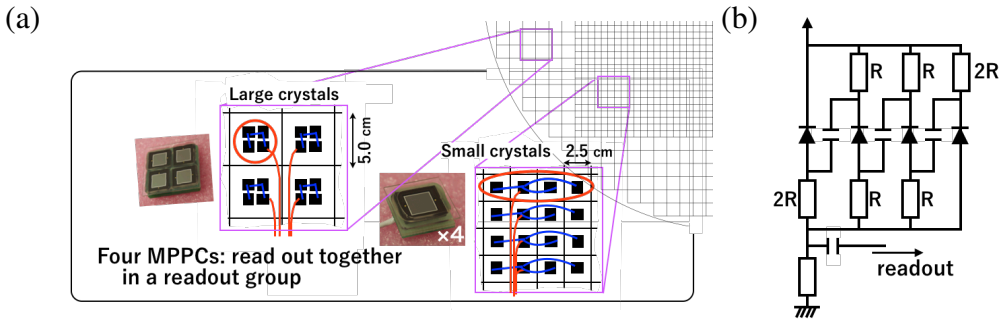

Figure 2: (a) Configuration of four SiPMs on large and small crystals. (b) Readout/Bias circuit for four SiPMs.

To merge signals from four SiPMs, we used a special circuit which effectively has parallel paths for biases and serial paths for signals, as shown in Fig. 2(b). This technique was originally developed for the MEG II experiment [5]. Other candidates had been a simple series-circuit of four SiPMs and the parallel connection of four SiPMs. The former method had a problem because the amount of irradiation depended on the distance from the beam line. If the amount of irradiation were different among the four SiPMs in the circuit, their dark current would start to differ, and the bias voltage on the SiPMs would change. Though the latter method solved the problem of bias depending on the irradiation, the timing resolution degraded by 30% even though a capacitance for each SiPM shortened the decay time constant.

2.3 Construction at J-PARC

There were five requirements for upgrading the calorimeter: 1) no air gap (bubble) between SiPM and the CsI surface, 2) gluing stronger than guarantee of contact retention of cable connectors of 4 N[2], 3) small

[1] https://www.hamamatsu.com/eu/en/product/type/S13360-6050CS/index.html
[2] U.FL-2LPHF6-068N2T-A, https://www.hirose.com

material budgets, 4) high vacuum (0.1 Pa) resistance and no outgas, and 5) installation without disassembling the calorimeter. We used glue to retain SiPMs on the calorimeter surface to minimize the material budget. We developed a special technique to glue SiPMs on the vertical front surface of CsI without disassembling the calorimeter, and without introducing air bubbles in glue. This method consisted of two steps as explaind in Fig. 3(a) and (b).

First, we glued SiPM(s) on a quartz plate with 14 × 14 × 0.5 mm^3 for a small crystal and 25 × 25 × 0.5 mm^3 for a large crystal with four SiPMs with a silicone TSE 3032 (TSE). TSE is transparent to 310 nm scintillation light, has no degradation toward neutron irradiation, and has been used for the silicon pads to connect PMTs to the CsI crystals. TSE was filled between SiPM and the quartz plate with an extra thickness of 200 μm. After curing at 45°C for 20 hours, we pressed SiPM against the quartz plate with 2N and fixed it with an epoxy type glue Araldite2011. This procedure left an internal pressure to TSE; it prevented small vacancies between the SiPM and the quartz plate appearing under low ambient temperature. We confirmed that the products were stable at the temperature ranging from -10°C and 45°C.

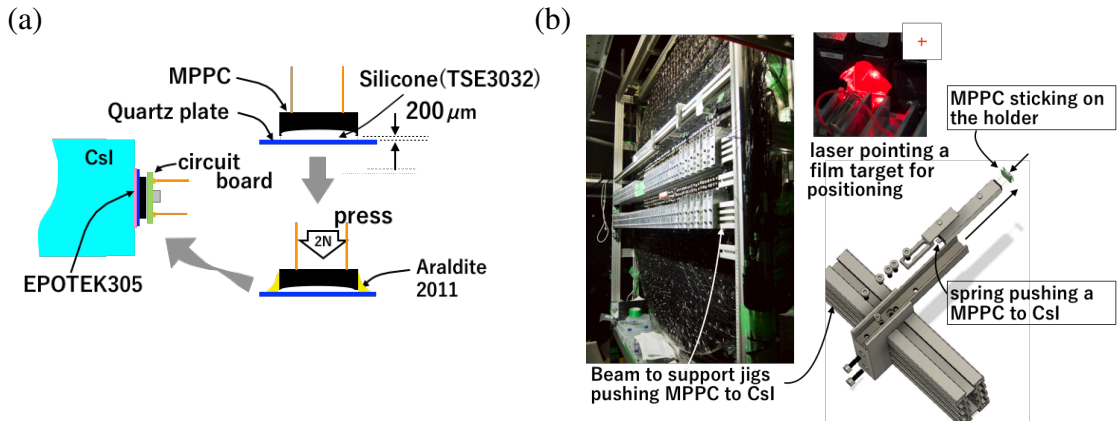

Figure 3: (a) Procedure to glue the SiPM on CsI surface. (b) Tools to glue the quartz plate on the CsI surface.

After soldering the circuit board shown in Fig. 2(b) to the SiPM and checking the breakdown voltage, dark current, photon yield, and the tolerance in 0.1 Pa, we proceeded to the next step. The second step, Fig. 3(b), is to glue SiPMs via the quartz plate on the surface of CsI crystals. An epoxy glue, EPOTEK 305 (EPOTEK) which is transparent to 310 nm, was selected for this purpose. A 12 mg of drop was dispensed on a quartz plate for small crystals and two of 12 mg drops were dispensed on a quartz plate for large crystals, and they were pushed toward the crystals with special jigs for 16 hours. After curing, a part of crystal surface surrounding the SiPM-quartz was covered with a reflector film made of aluminized polyethylene terephthalate. After cabling the circuit board, every crystal was covered with an acrylic cover and rewrapped with the original wrapping film and additional black insulating tape. The acrylic covers protect the SiPMs in case of an earthquake, and prevent aluminized wrapping film from shorting the circuit. The second step was held in a temporary-made dry room enveloping whole of the CsI calorimeter onsite in J-PARC, because the CsI crystals has a large hygroscopicity. Detail of gluing method has been reported in [6].

3. Performance

3.1 Analysis

A 10 pole Bessel filter converts raw electric signals from SiPMs to a Gaussian shape pulse, and the 125 MHz analog digital converter (ADC) [7] records the converted pulses. Most of the KOTO detector signals are recorded similarly[3] including signals from PMTs and SiPMs of the CsI calorimeter. The timing of a pulse was defined to be the time when the leading edge of the pulse exceeds a half of its maximum peak

[3]Signals of some detectors are recorded with 500 MHz ADC without using the Bessel filter.

height. The pulse height was determined as the peak of a parabola curve matching with the three highest data points. Each shower cluster is composed of multiple hits of crystals in a shower. We calculated Δ_T as $T_{\mathrm{SiPM}} - T_{\mathrm{PMT}}$, where T_{SiPM} is the energy-weighted average timing of SiPM signals in a cluster. Each deposited energy was measured by integrating the pulse shape of the corresponding PMT signals. T_{PMT} is the energy-weighted average of PMT signals of crystals in the cluster.

To study the response to gammas, a high-purity sample of gammas in $K_L \to 3\pi^0$ decays was collected by requiring six clusters on the calorimeter forming the reconstructed K_L mass between (498 $\pm$ 15) MeV/c^2. For neutrons, we conducted special runs in which 3-mm-thick aluminum plate was inserted in the neutral beam at the most upstream of the KOTO detector to scatter the neutrons.

3.2 Performance with the Δ_T

Out of two Δ_T's in two clusters in each event, the larger (smaller) Δ_T is referred to as Δ_T^{max} (Δ_T^{min}). Figure 4(a) (Fig. 4(b)) shows the distribution of Δ_T of two clusters for the gamma samples (neutron samples). Neutron clusters have larger Δ_T^{max} than gamma clusters.

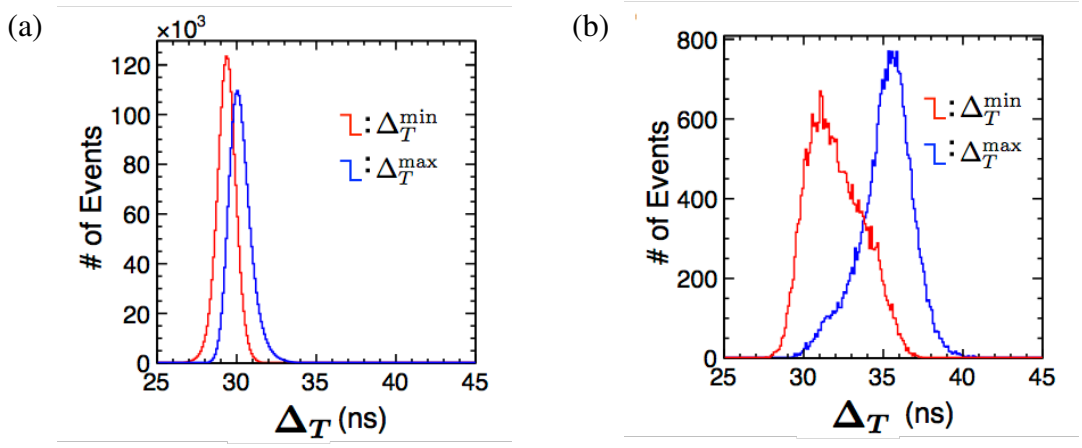

Figure 4: (a) Distributions of Δ_T for two gamma events, and (b) for neutron events.

Figure 5 shows the Δ_T^{max} of gamma events and neutron events. By requiring $\Delta_T^{\mathrm{max}} > 31$ ns, (97.9±0.1)% of neutrons are eliminated while 90% of gammas remained. The Δ_T has a correlation with the deposited energy in the crystals, and the distribution of the deposited energy of the $K_L \to \pi^0\nu\bar{\nu}$ events is higher than that of the $K_L \to 3\pi^0$ events. After correcting for the spectrum difference of the energy dependence, we estimated that (98.4±0.1)% of neutron events can be rejected while keeping 90% of gamma events. The expected number of neutron background events is 0.5 at the sensitivity to observe one $K_L \to \pi^0\nu\bar{\nu}$ event predicted by the SM.

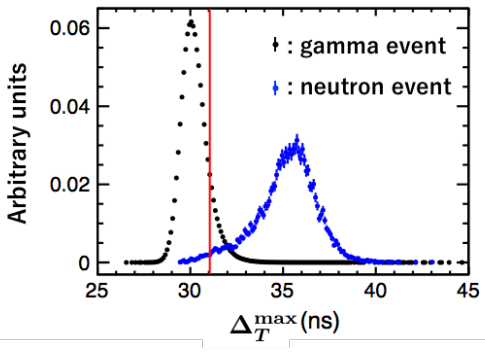

Figure 5: Distribution of Δ_T^{max} for two gamma events and neutron events, with a cut line keeping 90% of gamma events.

3.3 Performance with intrinsic time T_{inv}

The mean time of SiPM signal and PMT signal (T_{inv}) measures the timing information of a shower, whereas a Δ_T measures the shower depth. The second shower occurs after the primary one in neutron events, whereas both occur at the same time in the case of $\pi^0 \to \gamma\gamma$. Consequently, the absolute value of the

difference of $T_{\rm inv}$'s between two showers ($\Delta_{T_{\rm inv}}$) is larger in the neutron events than in the two-gamma events. Note that the difference tends to be canceled when we use only the timing in PMTs, because the propagation time of scintillation light from the shallow primary shower to PMT is comparable to the neutron propagation time from the primary shower to the second shower.

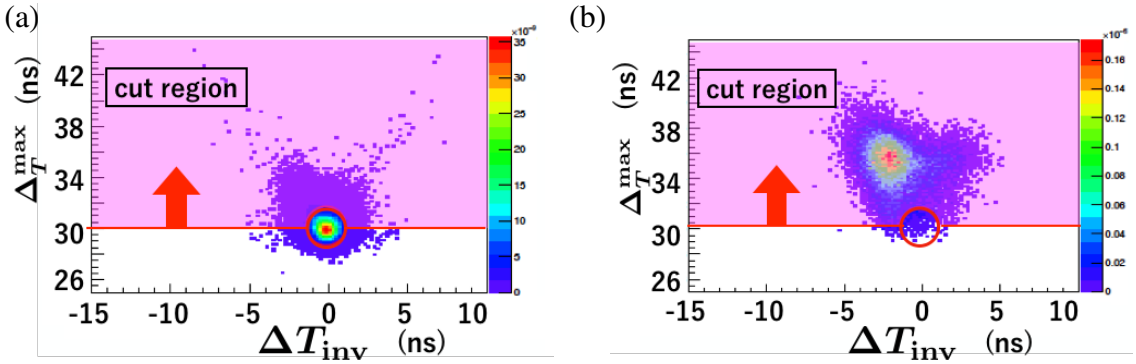

Figure 6: Distribution of $\Delta_T^{\rm max}$vs. $\Delta_{T_{\rm inv}}$ for the (a) gamma events and (b) neutron events.

Figure 6 shows the correlations between $\Delta_T^{\rm max}$ and $\Delta_{T_{\rm inv}}$ of two showers for the gamma events (a), and the neutron events (b). The neutron events having larger $\Delta_T^{\rm max}$ (deeper second shower) have negatively larger $\Delta_{T_{\rm inv}}$, whereas the gamma events are concentrated at $\Delta_{T_{\rm inv}} = 0$. When we use a criterion shown in Fig. 6, (99.04±0.06)% of neutron events are rejected while keeping 90% of gamma events. The expected number of neutron background events is 0.3 at the sensitivity to observe one $K_L \to \pi^0\nu\bar{\nu}$ event predicted by the SM.

4. Conclusion

We have developed a 4-D calorimetry to discriminate the neutron backgrounds from the signature of $K_L \to \pi^0\nu\bar{\nu}$ decays. For this purpose, we upgraded the calorimeter by gluing 4080 SiPMs on the front surface of the crystals.

We estimated that (99.04±0.06)% of neutron backgrounds can be rejected while keeping 90% of gamma events, when we use both $\Delta_T^{\rm max}$, depth information, and $\Delta_{T_{\rm inv}}$, timing information from the both-side readout calorimeter. This corresponds to 0.3 neutron background in the SM sensitivity of $K_L \to \pi^0\nu\bar{\nu}$.

References

[1] J. K. Ahn, Phys. Rev. Lett. **122**, 021802 (2019).

[2] L. S. Littenberg, Phys. Rev. **D 39**, 3322 (1989).

[3] V. Cirigliano, G. Ecker, H. Neufeld, A. Pich, and J. Portolés, Rev. Mod. Phys. 84, 399 (2012), and references therein.

[4] N. Hara, 2018 Proc. the 5th PD18 (Tokyo), JPS Conf. Proc. 27 (2019) 012012.

[5] A. M. Baldini *et al.*, Eur. Phys. J. C, 78: 380 (2018).

[6] K. Kotera, 2020 Proc. KAON 2019 (Perugia), J. Phys.: Conf. Ser. 1526 012036 DOI: 10.1088/1742-6596/1526/1/012036.

[7] S. Su *et al.*, IEEE Trans. Nucl. Sci., **64**, 1338-1345 (2017).